ORIGINAL RESEARCH ARTICLE

Flash Sintering of Rhenium in About 1 Minute with Electrical Current

EMMANUEL A. BAMIDELE, ALAN W. WEIMER, and RISHI RAJ

We show that rhenium can be sintered from powders to nearly full density (99.96 pct) by directly injecting electrical current into dogbone shaped specimens. The current was increased at a rate of 1 A s^{-1}. The specimen sintered abruptly after about 30 seconds when its temperature had risen to 900 °C. The experiments were carried out without furnace heating, within a glove box in Ar atmosphere. The following in-operando measurements are reported, (i) shrinkage strain with a rapid rate camera, (ii) resistivity measured by voltage and current, (iii) temperature measured with a pyrometer, and (iv) electroluminescence spectra measured with a spectrometer. The sintering cycle, the first, during which the sample sintered to full density, was followed by two more flash cycles with the same specimen. In the first cycle, the change in resistance exhibited a peak arising from abatement of interparticle interface resistance; the peak was absent in the second and third cycles. The rapid sintering is attributed to the generation of defects in the form of vacancy-interstitial (Frenkel) pairs. The concentration of the Frenkels was estimated from *in-situ* calorimetry, where the difference between the electrical input energy, and the energy lost to radiation, convection and specific heat, was attributed to an endothermic reaction for defect generation. In this way we calculated a concentration of ~ 10 mol pct of Frenkel pairs. The resistance of the flash sintered specimens was higher than literature values, presumably due to these defects. The very low sintering temperature and the anonymously high defect concentrations mean that flash sintering of metals is a far-from-equilibrium phenomenon.

https://doi.org/10.1007/s11661-024-07461-1

I. INTRODUCTION

WHILE experiments on flash sintering of ceramics[1,2] are now wide spread, its application to metals is quite recent. Field assisted sintering of tungsten carbide was reported in 2022.[3] Very recently tungsten powder has been shown to sinter at ~ 1000 °C by direct injection of current without furnace heating.[4] The hardness of these specimens was on par or better than specimens made by conventional methods. Two additional features of the tungsten-flash experiment were: (i) electroluminescence and (ii) evidence of an endothermic reaction which was attributed to the generation of defects, presumed to be Frenkel pairs. *In-operando* resistivity, measured as a function of temperature, deviated considerably from literature values. A much earlier work by McWilliams on field assisted sintering of aluminum powder,[5] although not recognized as such, may also have been a flash effect.

Current rate flash sintering of metals bears similarity to electro-discharge-sintering.[6] In EDS, a significant amount of energy, stored in a capacitor, is discharged into a powder-sample, causing it to sinter in less than a millisecond. The short time scale of EDS precludes characterization of features that are reported here where the sintering time was stretched out to several seconds. The high degree of control in the present experiment can advance scientific understanding of the flash phenomenon. It may also be technologically significant: for example, it can be instituted into additive manufacturing for producing ready to use parts without the need for oven sintering.

Re melts at 3182 °C. In conventional sintering, temperatures near $0.75T_M$ (*i.e.* 2318 °C) applied over several hours are needed. Instead, here we show that full sintering occurs at ~ 900 °C in approximately 30 seconds. The flash effect is accompanied by intense electroluminescence and an anomalous change in resistance with temperature. Additionally, we report calorimetric measurements of the enthalpy during the flash

EMMANUEL A. BAMIDELE is with the Materials Science and Engineering Program, University of Colorado at Boulder, Boulder, CO 80309. ALAN W. WEIMER is with the Department Chemical and Biological Engineering, University of Colorado Boulder, Boulder, CO, 80309. RISHI RAJ is with the Materials Science and Engineering Program, University of Colorado at Boulder and also with the Department of Mechanical Engineering, University of Colorado at Boulder, Boulder, CO 80309-0427. Contact e-mail: rishi.raj@colorado.edu
Manuscript submitted January 5, 2024; accepted May 20, 2024.
Article published online August 2, 2024

process (measured as the excess of electrical energy over the energy loss from radiation, convection and specific heat); it shows the presence of an endothermic reaction, which is ascribed to the generation of point defects, assumed to be Frenkel pairs. Ultrahigh concentration of these defects, approximately ~ 10 mol pct, are estimated in this way.

II. METHOD

Rhenium powders with a purity of 99.99 pct and a particle size of − 325 mesh, were supplied by Fisher Scientific. About 1 g of the powder, without binders, was pressed in a die to produce dogbone-shaped samples, with the use of a hydraulic press (Dake Corporation) at a pressure of 140 MPa. The specimen measured $16 \times 3.12 \times 0.44$ mm^3 (gage length × width × thickness). Using the Archimedes method, we determined the green density, ρ_g to be ~ 74 pct.

The electrical current was supplied by Hewlett Packard 6261B power supply (0 to 20 V, 0 to 50 A). Tungsten electrodes, 1 mm in diameter, were inserted through 1.1 mm diameter holes located in the ears of the dogbone specimens. The current was injected at a constant rate of 1 A s^{-1} using a method adapted from Kumar *et al.*[7] A home-built software was interfaced to the hardware *via* a National Instrument data acquisition device (NI DAQ). The voltage, the temperature and the current were recorded continuously as the current was increased at a constant rate.

The experiments were carried out at ambient temperature inside an argon-filled glovebox made by Vacuum Atmosphere Company. The argon gas, 99.9 pct pure, was provided by Airgas, maintaining O_2 partial pressure at 20 to 100 ppm.

The resistance was measured with a four point probe. The voltage probes were placed within the gage length of the dogbone, a distance of 6.9 mm apart. The voltage was measured with a Keithley digital multimeter. The resistance in Ω was determined from the *I–V* curve. The resistivity, in units of Ωcm, was obtained by multiplying the resistance with the cross-sectional area and dividing by the distance between the voltage probes. The experiment's layout is depicted in Figure 1.

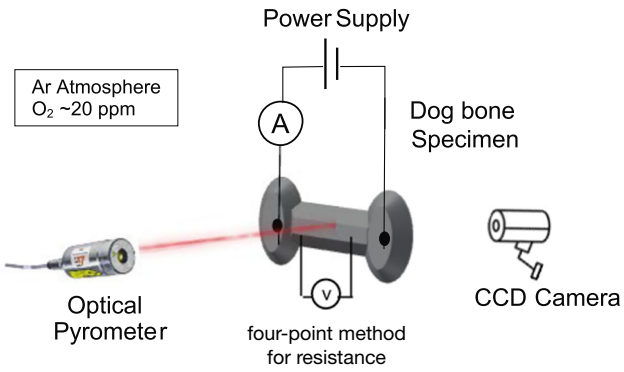

Fig. 1—Flash sintering of metals without a furnace.

The rate of shrinkage of the specimen was obtained from pictures taken at the rate of 10 frames per second with a CCD camera (Imaging Source, Germany). The video was processed with Fiji software to determine the shrinkage. The temperature was measured with a CLTM-1HCF4-C3 pyrometer, manufactured by Micro-Epsilon. This pyrometer operates within a temperature range of 400 °C to 1200 °C. Emissivity was configured at 0.3.[8,9]

III. RESULTS

A. *Sintering*

The flash sintering experiment was conducted by increasing the current at a rate of 1 A s^{-1}. The corresponding shrinkage curve is presented in Figure 2. The duration required for full sintering was 34 seconds. The sintered density can be calculated from the formula $\rho_g = \exp(3\epsilon_1)$.[10] Here, ρ_g stands for the initial (green) density, ρ represents the time dependent density. ϵ_1 denotes the linear shrinkage strain (it is a negative value). Therefore, with a shrinkage strain of − 0.09 and an initial density of 74 pct, the sinter density is estimated to be 97 pct; the Archimedes density was measured to be 99.6 pct.

B. *Microstructure*

Microstructures of the specimens before and after sintering obtained in the SEM, are shown in Figure 3. The Archimedes density of the green sample was 74 pct and that of the flash-sintered sample was 99.6 pct.

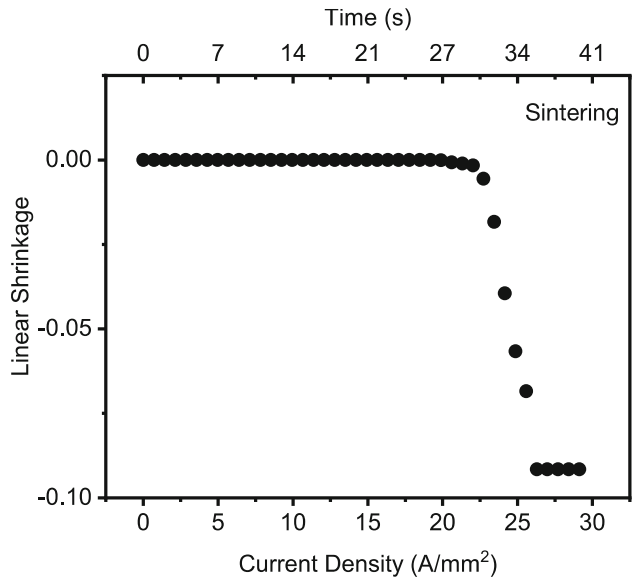

Fig. 2—Sintering strain as a function of the current density in the powder pressed dogbone sample.

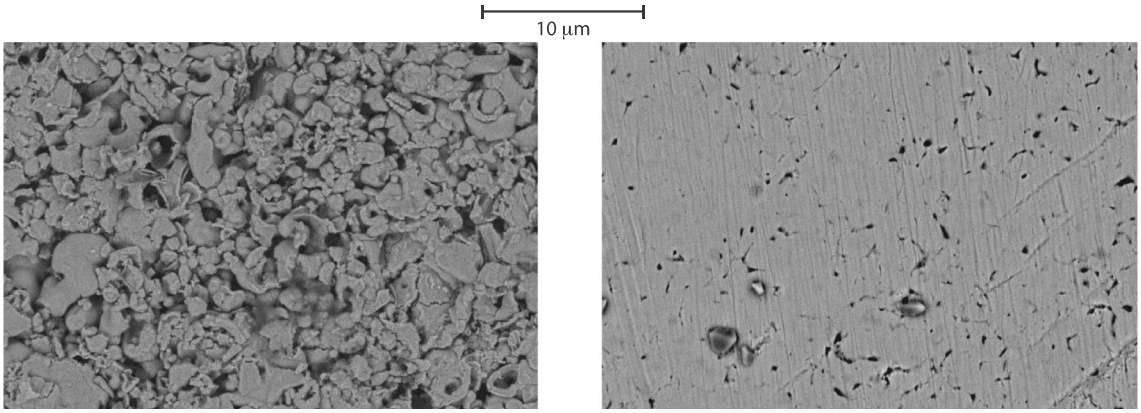

Fig. 3—Microstructure before and after sintering.

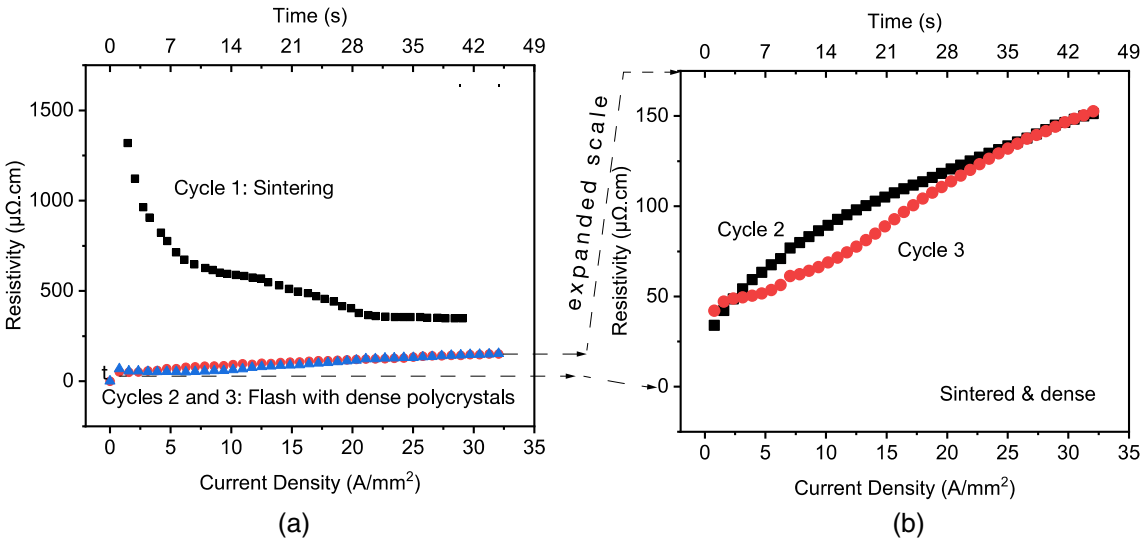

Fig. 4—(*a*) The change in resistance with current density. The first cycle refers to the sintering of the powder pressed sample. Cycles 2 and 3 were repeated on this sintered specimen. (*b*) Resistance shown with expanded resistivity scale for cycels 2 and 3.

C. *Three Cycles*

The resistivity of the specimen was measured in real time during the sintering experiment, when the specimen starts as a powder compact, and then again after sintering when the specimen is a dense polycrystal; both conducted with the same current density. The first measurement is called Cycle 1; the measurements from the dense polycrystals repeated twice are called Cycle 2 and Cycle 3.

The change in resistivity with current density for the three Cycles are plotted in Figure 4. During Cycle 1 the compacted powder is sintered. The transient peak during this Cycle is attributed to the removal of the interparticle resistance. It is absent during Cycle 2 and Cycle 3 since the specimens are now dense polycrystals. Note that the results from Cycle 2 and Cycle 3 are self-consistent. A similar phenomenon was seen in experiments with aluminum powders[5] and in tungsten.[4]

D. *Temperature and Luminescence*

The change in temperature and the progression of electroluminescence with the current density, measured during Cycle 2, are shown in Figure 5. The temperature was measured with the pyrometer and the luminescence with the spectrometer (in the same experiment).

The optical emission is attributed to electroluminescence, as opposed to black body radiation, for a couple of reasons: (i) the temperatures measured (< 1000 °C) are too low for optical emission from Joule heating, and (ii) the emission peak's intensity increases with rising specimen temperature but its position remains unchanged with respect to wavelength. In black body radiation the emission peak shifts towards shorter wavelengths as temperature rises.

Electroluminescence is a key feature of flash sintering in ceramics. In metals it is unexpected: the electronic conductivity of metals was expected to quench the photons. But on further thought, the flash event is ceramics, which are nominally insulators, is also

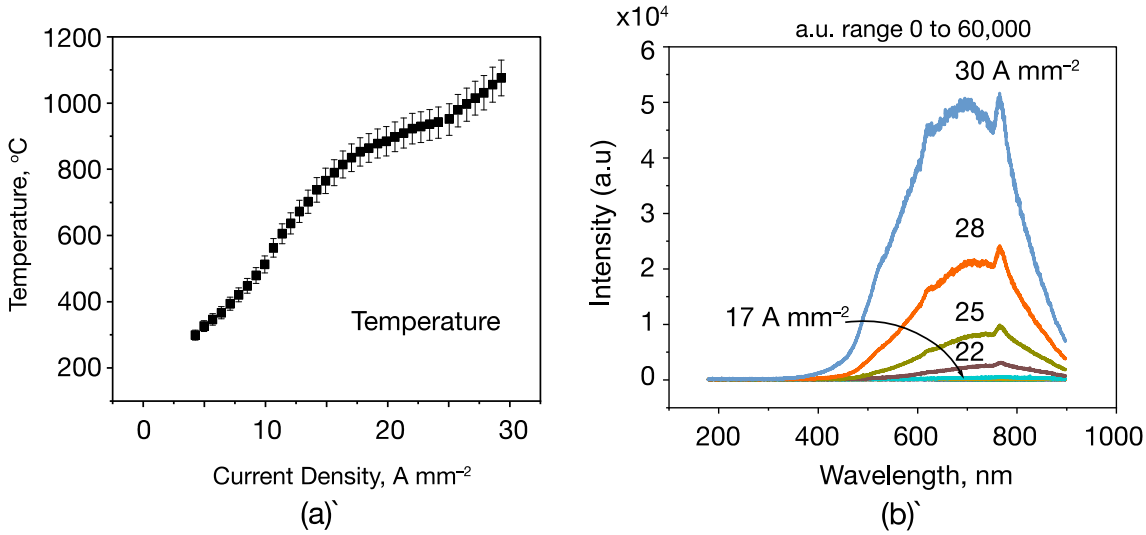

Fig. 5—(*a*) The change in the specimen temperature with current density. (*b*) Optical emission spectrum at different current densities. Luminescence at ~ 17 A mm^{-2} is attributed to the onset of flash.

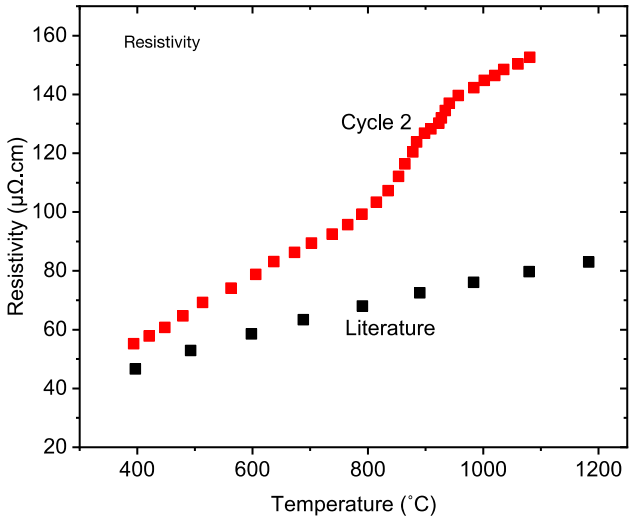

Fig. 6—Change in resistance (red) with temperature in comparison to literature values (black[11]). The resistance during flash is higher because of defects. The rate of defect generation apparently accelerates at higher current densities (Color figure online).

accompanied by a transition to electronic conductivity; so perhaps its presence in metals is not so unusual. Nevertheless these results provide new information about understanding the fundamental origin of electroluminescence in flash experiments, which, so far, remains controversial.

E. *The Resistivity*

The in-operando resistance measured using the four-point technique, described in Section II, is shown in Figure 5. The measurement from cycle 2 is compared with the literature values which are represented in black color. Figure 6.[11]

The temperature dependent resistivity data from the flash experiment are higher than the data from the literature.[11] This difference arises from defects that are generated during the flash experiment. The effect is stronger at higher temperature (higher current densities) which further supports this interpretation since current density has been found to be a key parameter in the generation of defects.[12] Note that the resistance profile during flash shows two inflexions, the first at 800 °C and the next at 1000 °C. In the next section we show that the inflexions coincide with a change in the rate of defect generation. The precise reason why is not understood; it is thought to be related to the change in the spatial distribution of defects which can be expected to influence the scattering of electrons.

F. *Calorimetry: Endothermic Enthalpy*

A consistent observation in flash experiments is a deficit between the input electrical energy and the energy calculated from losses attributed to radiation, convection, and specific heat. This disparity "energy deficit," provides a method for determining endothermic defect concentrations; obtained by dividing the energy deficit by the enthalpy of defect formation enthalpy.[7,13]

The energy deficit, denoted as $\Delta H^*(t)$ in Joules, is given by the following expression:

$$\Delta H^*(t) = \int_0^t (W - W^*)dt \qquad [1]$$

where, $W(t)$ is the electrical energy (measured in Watts) expended in the specimen, and $W^*(t)$ is the sum of watts lost to radiation, convection, and specific heat. $W(t)$ is obtained from the product of the current and the voltage. Note that these parameters vary with time. The losses attributed to radiation, convection,

and specific heat are derived using the following expressions[7,13]:

$$W^*(t) = W^*_{\text{BBR}}(t) + W^*_{\text{conv}}(t) + W^*_{\text{spht}}(t) \quad [2]$$

$$W^*_{\text{BBR}}(t) = \in_m S\sigma\left(T_K^4 - 298^4\right), \quad [3]$$

$$W^*_{\text{conv}}(t) = hS(T_K - 298), \quad [4]$$

$$W^*_{\text{spht}}(t) = mC_p \frac{dT_K}{dt} \quad [5]$$

where the terms on the right-hand side of Eq. [2] refer to the energy lost to black body radiation, to convection and to specific heat. In Eq. [3], S is the specimen surface area, $\in_m$ is the emissivity of Re (0.3), and σ is the Stefan-Boltzmann's constant (5.6704×10^{-8} W m^{-2} K^{-4}); 298 K is the ambient temperature within the glove box. Equation [4] is discussed further just below. In Eq. [5] m is the specimen mass (0.00035 kg), and C_p, the specific heat, equal to 137 J kg^{-1} K^{-1}. T_K is the specimen temperature in Kelvin. Note that Eq. [2] is in units of Watts (J s^{-1}): it is integrated with respect to time to obtain the energy deficit in J.

The parameter h, in Eq. [4] is the convective heat transfer coefficient. It depends on many factors such as surface chemistry and morphology, gas velocity at the interface, and the heat capacity of the gas, which depends on pressure and the specific heat. For example, Argon has a significantly lower heat capacity than nitrogen. Therefore, the heat transfer coefficient in Ar will be lower than in air. Therefore, its value varies over a wide range; in air ranges from 10 to 100 W m^{-2} K^{-1}.

The value for h was estimated by the following method. It is related to convection losses which are expected to increase linearly with temperature. In contrast the black body radiation (BBR) loss scales as T^4. This means convection is dominant at lower temperatures but is overtaken by BBR at higher temperatures. The commonly accepted cross-over temperature, where energy loss transitions from convection to BBR, is approximately 600 °C. This point is typically when the emitted light exhibits a faint red hue. A corresponding graph using our data is presented in Figure 7, shows that the transition occurs near 600 °C when h = 20 W m^{-2} K^{-1}. This is the value we use for calculating the energy deficit in Eq. [1].

In order to calculate the mole fraction of defects it is necessary to express ΔH^* in moles. We begin with calculating the moles of *Re* in the specimen. Dividing the specimen volume by the molar volume of *Re* gives the number of moles of *Re* in the specimen, N_W, that is

$$N_W = \frac{V_{\text{specimen}}}{V_{\text{molar}}} \quad [6]$$

The enthalpy in Eq. [1] may now be written in moles:

$$\Delta H^*_{\text{mol}} = \frac{\Delta H^*}{N_W} \quad [7]$$

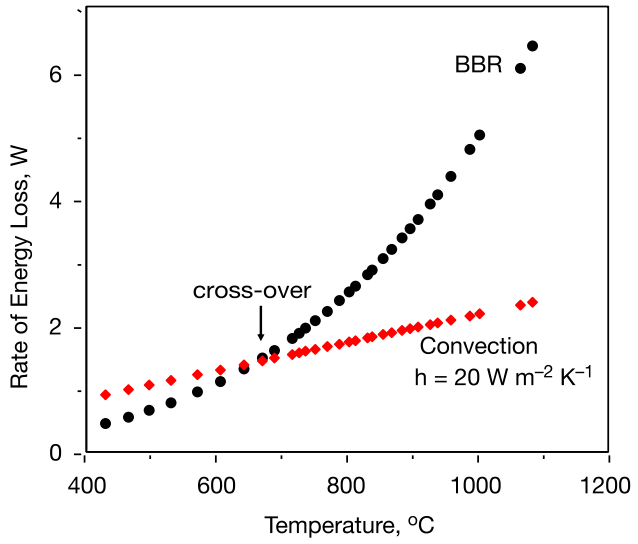

Fig. 7—The cross over from convection to black body radiation dominated loss at 600 °C which occurs for h = 20 W m^{-2} K^{-1}.

To calculate the mole fraction of defects Eq. [7] is divided by the formation energy of the defects in J mol^{-1}, which has been obtained from embedded atom potential in molecular dynamics simulation.[14] The mole fraction of defects is then given by

$$x_F = \frac{1}{E_F}\frac{\Delta H^*}{N_W} \quad [8]$$

Here, E_F is the formation energy of Frenkel defects in units of Joules mol^{-1}.

Substituting for $V_{\text{specimen}} = 22.5 \times 10^{-3}$ cm^3 and $V_{\text{molar}} = 8.67$ cm^3 mol^{-1}, and $E_F = 11.96$ eV into Eqs. [6] through [8], after converting E_F from eV to J mol^{-1} (by multiplying by 96,500 J eV^{-1}), gives the molar concentration of defects. The details of the numerical analysis are given below.

Implementing the above procedures leads to the data given in Table I, in the following steps:

1. The input data are the temperature and electrical power input as a function of time.
2. The left-hand side of Eqs. [5] through [7] are obtained by inserting the temperature data into the right-hand side.
3. The watt measurements are converted to Joules through time integration.
4. Energy loss is calculated by combining BBR, convection and specific heat data.
5. The total energy loss is subtracted from the input energy to give ΔH^*.
6. Next Eq. [8] gives the mole fraction of Frenkel defects. They are given in the right hand most column in Table I.

Plots for the energy deficit in kJ mol^{-1}, and the mole fraction of Frenkel pairs are plotted in Figures 8(a) and (b). The defect concentration rises to 10 pct mole fraction. Comparatively, values calculated from thermal

equilibrium are many, many orders of magnitude lower. Experiments with tungsten, also a refractory metal with a very high melting point also gave a rather high value of 26 pct.

The pattern of flash sintering observed in the present study is similar to tungsten[4] in other respects as well. In both instances the resistance is higher than literature values, pointing to the role of defects. The profiles for different parameters exhibit three regimes shown in Figure 9. The pattern starts with an incubation time, followed by the onset of electroluminescence, and finally by sintering.

IV. DISCUSSION

Flash sintering of ceramics was first reported in 2010. It has three characteristics: colossal rates of sintering (in a few seconds at temperatures well below conventional sintering),[2] a transition to electronic conductivity (even in ionic and insulating ceramics),[15,16] and electroluminescence.[17] In oxides the proliferation of oxygen vacancies have been held responsible for this unusual phenomenon.[18] Therefore, the idea of flash sintering of metals had not been thought to be feasible. Furthermore, it was not reasonable to expect electroluminescence in metals where electronic conductivity would be expected to quench the photons.

The present work on metals is a new development in the field of flash sintering, which so far has been mostly applied to ceramics. Nominally, a refractory metal, such as tungsten, requires ultrahigh temperatures for several hours in inert environments to achieve densification. To our great surprise these flash experiments were successful: tungsten could be sintered to full density in mere seconds at ~ 1000 °C. Indeed they could be carried out without a furnace by heating the specimen by directly injecting current and increasing it at a constant rate. Here we show that flash can extend to other metals, *Re*, as reported here and Ni as reported elsewhere recently.[19]

The results for *Re* are similar to those in tungsten. Both have similar melting points: 3182 °C for Re and 3383 °C for W. Solid state diffusion theories link the diffusion coefficient to the melting point of the metal.[20] Generally sintering occurs at $0.75T_M$ (2318 °C) over a period of several hours. In comparison, the current rate flash sintering occurs near 900 °C to 1000 °C in about one minute, for both W and *Re*. Both metals sintered at a current density of 20 to 24 A mm^{-2} (for similar workpiece geometry).

In-situ calorimetry which measures the energy deficit, equals difference between the input electrical energy and the energy lost to radiation, convection and specific heat, is interpreted as an endothermic reaction for the generation of point defects. The colossal concentration of these point defects (calculated as Frenkel pairs) partly explains the high rates of solid-state diffusion that must underpin the ultrafast sintering rates. Similar measurements have been made during flash sintering of oxides.[4,13] In both metals and ceramics, flash is a far-from-equilibrium phenomenon.

Diffusion coefficients are products of defect concentration and the mobility of atoms. The high diffusivity may be attributed to the concentration of defects. Indeed, real-time measurements of diffusion coefficients across bilayers in ceramics suggest that diffusion rates in flash are almost $\times 10^8$ times faster.[21] The activation energy for diffusion are found to be one half of the values in literature.[22] Generally the activation energy for diffusion is the sum of two quantities: the energy of formation of defects and the activation energy for atom jumps. Since in flash, the defect concentration is very high, only the activation energy for atom jumps would appear in the diffusion coefficient. Bilayer experiments with two metals for measuring the coefficients of diffusion are recommended.[21]

It is to be noted that the features of flash (ultrafast diffusion, electroluminescence and the "energy deficit") occur not only during sintering of powders but also in dense polycrystals. This result is the same as in ceramics where polycrystals, and single crystals,[23] have been shown to exhibit the typical characteristics of flash.

A rather surprising result is the presence of electroluminescence in metals. It is a key feature of flash in ceramics. But oxide ceramics, such as zirconia and yttria are wide bandgap materials where flash has been shown to create new energy levels below the conduction band that leads to band gaps that are consistent with the peaks in the electroluminescence spectrum.[24] Metals are zero band gap materials, therefore electroluminescence in W, Ni and *Re* is quite unexpected. This finding raises new questions about the fundamental origin of electroluminescence in flash experiments.

Ceramics and metals share one important common feature. Present experiments were carried out at different current rates where current injected into the specimen is increased at a constant rate. The rates are changed over a wide range, from one experiment to another. In ceramics, also, current rate experiments have been carried out at different rates, that vary over a factor of one hundred.[7] In both instances the sintering data collapse to a single master curve when the results are plotted not as a function of time but as a function of the current density. The same result is obtained here. Thus, importantly, it can be inferred that in both ceramics and in metals the defect generation is related to the current density.

The change in resistance during flash in metals is different than in ceramics. Ceramics, which are nominally not electronically conducting, show an abrupt rise in conductivity at the onset of flash; this transition to high current is controlled by switching the power supply to current control. However, experiments have also been carried out continuously under current control, by injecting current into the ceramic specimen, held at an elevated temperature, and increasing the current at a constant rate.[7] These experiments show a peak in the voltage (*i.e.* the resistance) corresponding to the onset of flash.

The present experiments with metals are carried out at different current rates, without a furnace since the specimen temperature rises spontaneously by Joule heating. In metals, that are intrinsically electronically

Table I. Frenkel Defect Analysis Based on Energy Deficit

Time (s)	Pyrometer Temp	Power Input	BBR (Watts)	BBR (Joule)	Conv. (Watts)	Conv.(Joules)	Spec. Heat (Joules)	Total IN (Joules)	Total LOSS (Joules)	Deficit per mole	Frenkel
sec	°C	W	W	Total J	W	Total J	Total J	J	J	kJ/mol	mol fraction
10	399	3.21	0.38	3.80	0.64	6.4	17.9	32.1	30.3	0.7	0.0006
11	429	3.88	0.46	4.25	0.69	7.1	19.4	36.0	33.1	1.2	0.0010
12	464	4.61	0.56	4.81	0.75	7.8	21.1	40.6	36.3	1.7	0.0015
13	496	5.24	0.66	5.47	0.80	8.6	22.6	45.8	39.6	2.5	0.0022
14	530	6.12	0.79	6.26	0.86	9.5	24.2	52.0	43.1	3.5	0.0031
15	570	7.04	0.96	7.23	0.93	10.4	26.1	59.0	47.3	4.7	0.0041
16	605	7.94	1.14	8.36	0.99	11.4	27.8	66.9	51.4	6.2	0.0054
17	641	8.38	1.34	9.70	1.05	12.5	29.5	75.3	55.9	7.8	0.0068
18	670	9.20	1.52	11.22	1.10	13.6	30.9	84.5	60.2	9.8	0.008
19	688	9.80	1.64	12.85	1.13	14.7	31.8	94.3	64.3	12.1	0.010
20	715	10.38	1.83	14.69	1.18	15.9	33.1	104.7	69.0	14.4	0.012
21	726	10.94	1.91	16.60	1.20	17.1	33.6	115.6	73.0	17.2	0.015
22	736	11.86	1.99	18.59	1.21	18.3	34.1	127.5	77.1	20.3	0.018
23	751	12.58	2.12	20.71	1.24	19.5	34.8	140.1	81.6	23.5	0.020
24	769	13.15	2.27	22.98	1.27	20.8	35.7	153.2	86.4	26.9	0.023
25	788	14.08	2.44	25.42	1.30	22.1	36.6	167.3	91.5	30.5	0.026
26	803	14.90	2.58	28.00	1.33	23.4	37.3	182.2	96.6	34.5	0.030
27	812	15.44	2.67	30.67	1.34	24.8	37.7	197.6	101.5	38.7	0.034
28	831	15.01	2.86	33.53	1.38	26.2	38.6	212.7	107.1	42.5	0.037
29	838	15.72	2.94	36.47	1.39	27.6	39.0	228.4	112.2	46.8	0.041
30	855	16.41	3.12	39.59	1.42	29.0	39.8	244.8	118.0	51.0	0.044
31	868	17.05	3.27	42.86	1.44	30.4	40.4	261.8	123.8	55.5	0.048
32	884	17.92	3.46	46.32	1.47	31.9	41.2	279.8	130.0	60.3	0.052
33	896	18.81	3.60	49.92	1.49	33.4	41.8	298.6	136.2	65.4	0.057
34	908	19.72	3.75	53.68	1.51	34.9	42.3	318.3	142.5	70.7	0.061
35	927	22.05	4.00	57.68	1.54	36.4	43.3	340.3	149.5	76.8	0.067
36	938	24.48	4.15	61.83	1.56	38.0	43.8	364.8	156.3	83.9	0.073
37	959	26.27	4.45	66.28	1.60	39.6	44.8	391.1	163.8	91.5	0.079
38	988	26.22	4.88	71.17	1.65	41.2	46.2	417.3	172.3	98.6	0.085
39	1003	26.52	5.12	76.29	1.67	42.9	46.9	443.8	180.4	106.0	0.092
40	1065	28.00	6.20	82.48	1.78	44.7	49.9	471.8	191.9	112.7	0.098
41	1084	29.93	6.56	89.04	1.81	46.5	50.8	501.8	201.8	120.7	0.105

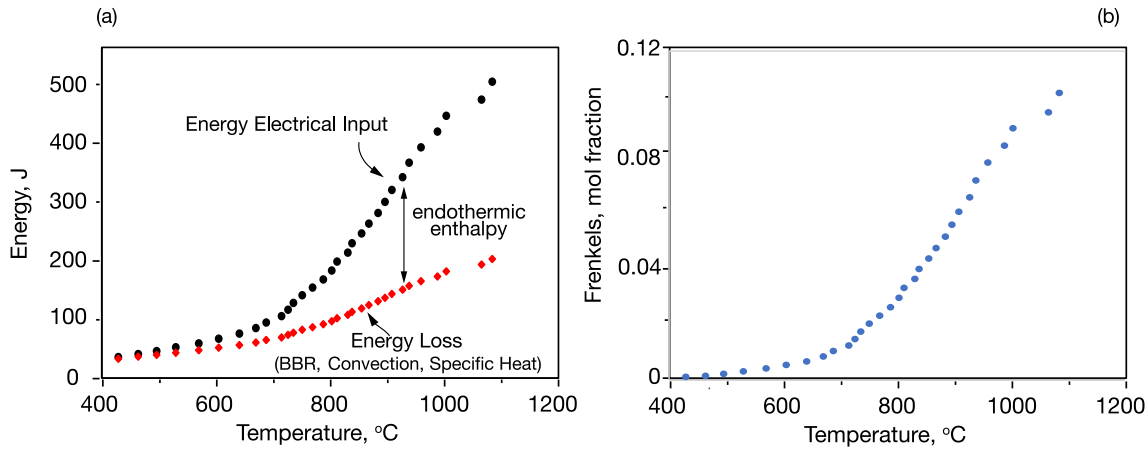

Fig. 8—(*a*) Plots of the energy deficit as given by Eqs. [1] through [5]. The energy input is greater than the energy dissipation indicating an endothermic reaction. (*b*) The energy deficit is converted into defect concentration by dividing by E_F the energy of formation of Frenkles.

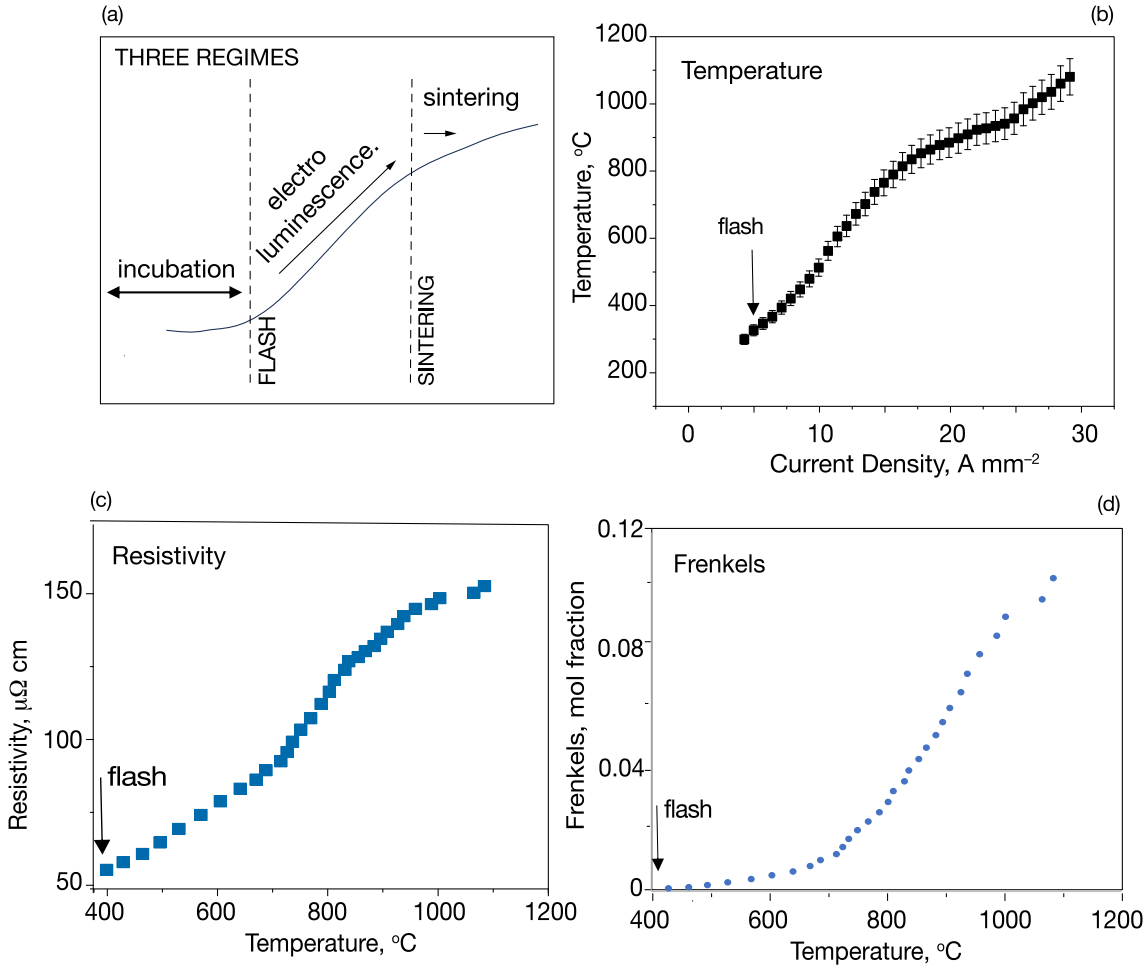

Fig. 9—Phenomenological behavior of flash in metals showing the onset of flash, sintering, temperature and resistivity with increasing current density. The temperature is plotted with respect to current density, and the defects and resistivity with respect to temperature.

conducting, the onset of flash is expressed in a different way than in ceramics. The change in resistance has a different pattern. In general these data, presented as the change in resistance with temperature (which is measured with a pyrometer) show values that are quite different from literature. In metals, unlike ceramics, the resistance increases with temperature. However, the change in resistance with temperature, and their absolute values are quite different from handbook data. First, the magnitude of the resistivity is higher which can be ascribed to the generation of point defects. But the change with temperature is far from being approximately linear as traditionally expected. The shape shows transitions, first at the onset of electroluminescence, and then when the sample abruptly sinters. The onset electroluminescence can be ascribed to the onset of a flash. After this transition the rate of increase in resistance with temperature is slower than handbook data, implying an effective increase in conductivity, which is somewhat akin to the behavior of ceramics.

In summary, a comparison between flash experiments of metals and ceramics leads to the following observations: (i) colossal rates of sintering that point to equally high rates of self-diffusion in both metals and in ceramics, (ii) both cases exhibit electroluminescence, (iii) current rate experiments on both classes of materials, carried out at vastly different rates show that sintering is related to the instantaneous values of the current density, not to the rate at which it is increased, (iv) in both ceramics and metals the flash experiments reveal a significant energy deficit that translate into endothermic generation of defects, which are of colossal concentration suggesting that flash is a far-from-equilibrium phenomenon, and (v) the in-operando change in resistance in metals does not follow the conventional behavior in metals where the resistance increases monotonically with temperature; instead it shows two transitions, one at the onset of electroluminescence, and a second when the specimens sinter abruptly.

V. CONCLUSIONS

The experiments on flash sintering of W and now *Re*, provide interesting common features. Since they have similar melting points they show similar flash sintering behavior. Both metals sinter at 900 °C to 1000 °C. Both show, approximately, a sigmoidal behavior in the

resistance profile with respect to temperature. It consists of three phases, initially the profile is nearly flat, then rises sigmoidally and then tends to flatten again at higher temperatures. The phenomenological evidence suggests that this behavior is related to the generation of Frenkel pairs, as shown in Figure 8.

Apart from the new scientific questions raised above, flash sintering of metals may create new technological opportunities. For example, *in-situ* additive manufacturing of metal workpieces that do not require further sintering can be produced.

In ceramics, reactive flash sintering of elemental oxide powders that grow into a single phase multicomponent ceramic with unusual properties has been demonstrated.[25,26] A similar approach applied to high entropy metals and other alloys designed for super mechanical properties produced by unusual precipitation strengthening, may be feasible.

The ''flash eco-system'' has additional novel properties. Flash has been shown to produce far from equilibrium phases; that is, phases that do not fit classical thermodynamic behavior.[27] For example, such findings hold the possibility of new solid-state electrolytes for $Li+$ batteries, with high ionic conductivities.[26]

ACKNOWLEDGMENTS

This work was supported by a grant from NASA, ESI Program under the Grant Number 80NSSC21K0225. This grant urged us to try flash sintering of metals; we are grateful for that. We appreciate lively discussions with Dr. Jhonathan Rosales, and his encouragement as the work progresses. The rhenium powders used in this study were provided by Davis Conklin.

CONFLICT OF INTEREST

On behalf of all authors, the corresponding author states that there is no conflict of interest.

REFERENCES

1. R. Raj: *J. Am. Ceram. Soc.*, 2016, vol. 99, pp. 3226–32.
2. M. Cologna, B. Rashkova, and R. Raj: *J. Am. Ceram. Soc.*, 2010, vol. 93, pp. 3556–59.
3. I. Mazo, A. Molinari, and V.M. Sglavo: *Mater. Des.*, 2022, vol. 213, p. 110330.
4. E. Bamidele, S.I.A. Jalali, A.W. Weimer, and R. Raj: *J. Am. Ceram. Soc.*, 2024, vol. 107, pp. 817–29.
5. B. McWilliams, J. Yu, F. Kellogg, and S. Kilczewski: *Metall. Mater. Trans. A*, 2017, vol. 48A, pp. 919–29.
6. M.S. Yurlova, V.D. Demenyuk, LYu. Lebedeva, D.V. Dudina, E.G. Grigoryev, and E.A. Olevsky: *J. Mater. Sci.*, 2014, vol. 49, pp. 952–85.
7. P. Kumar, D. Yadav, J. Lebrun, and R. Raj: *J. Am. Ceram. Soc.*, 2019, vol. 102, pp. 823–35.
8. J. McClure, K. Boboridis, and A. Cezairliyan: *Int. J. Thermophys.*, 1999, vol. 20, pp. 1137–48.
9. U. Köster, T. von Egidy, H. Faust, T. Friedrichs, M. Groß, D. Habs, O. Kester, E. Steichele, and P. Thirolf: *Nucl. Instrum. Methods Phys. Res. Sect. B*, 1997, vol. 126, pp. 253–57.
10. R. Raj: *J. Am. Ceram. Soc.*, 1982, vol. 65, pp. C46–C46.
11. B.D. Bryskin: *Am. Inst. Phys.*, 1992, vol. 246, pp. 278–91.
12. J.S.C. Francis and R. Raj: *J. Am. Ceram. Soc.*, 2013, vol. 96, pp. 2754–58.
13. T.P. Mishra, R.R.I. Neto, R. Raj, O. Guillon, and M. Bram: *Acta Mater.*, 2020, vol. 189, pp. 145–53.
14. G. Bonny, A. Bakaev, D. Terentyev, and Yu.A. Mastrikov: *J. Appl. Phys.*, 2017, vol. 121, p. 165107.
15. A.R. West: *J. Mater. Chem. A*, 2023, vol. 11, pp. 12681–94.
16. S. Jo and R. Raj: *Scripta Mater.*, 2020, vol. 174, pp. 29–32.
17. K. Terauds, J.-M. Lebrun, H.-H. Lee, T.-Y. Jeon, S.-H. Lee, J.H. Je, and R. Raj: *J. Eur. Ceram. Soc.*, 2015, vol. 35, pp. 3195–99.
18. N. Masó and A.R. West: *Chem. Mater.*, 2015, vol. 27, pp. 1552–58.
19. E.A. Bamidele, M.M. Mahmoud, and R. Raj: *J. Am. Ceram. Soc.*, 2024, vol. 107, pp. 3659–65.
20. P.G. Shewmon: *Diffusion in Solids*, McGraw-Hill, New York, 1963.
21. S.I.A. Jalali and R. Raj: *J. Am. Ceram. Soc.*, 2022, vol. 106, pp. 867–77. https://doi.org/10.1111/jace.18804.
22. H. Motomura, D. Tamao, K. Nambu, H. Masuda, and H. Yoshida: *J. Eur. Ceram. Soc.*, 2022, vol. 42, pp. 5045–52.
23. X. Vendrell and A.R. West: *J. Electrochem. Soc.*, 2018, vol. 165, pp. F966–F975.
24. D. Yadav and R. Raj: *J. Am. Ceram. Soc.*, 2017, vol. 100, pp. 5374–78.
25. X. Vendrell, D. Yadav, R. Raj, and A.R. West: *J. Eur. Ceram. Soc.*, 2019, vol. 39, pp. 1352–58.
26. T. Clemenceau and R. Raj: *MRS Commun.*, 2022, https://doi.org/10.1557/s43579-022-00162-z.
27. J.-M. Lebrun, T.G. Morrissey, J.S. Francis, K.C. Seymour, W.M. Kriven, and R. Raj: *J. Am. Ceram. Soc.*, 2015, vol. 98, pp. 1493–97.